Vol. 23 • No. 47 • December 17 • 2013

www.afm-journal.de

ADVANCED FUNCTIONAL MATERIALS

WILEY-VCH

Composite Three-Dimensional Woven Scaffolds with Interpenetrating Network Hydrogels to Create Functional Synthetic Articular Cartilage

I-Chien Liao, Franklin T. Moutos, Bradley T. Estes, Xuanhe Zhao, and Farshid Guilak**

The development of synthetic biomaterials that possess mechanical properties mimicking those of native tissues remains an important challenge to the field of materials. In particular, articular cartilage is a complex nonlinear, viscoelastic, and anisotropic material that exhibits a very low coefficient of friction, allowing it to withstand millions of cycles of joint loading over decades of wear. Here, a three-dimensionally woven fiber scaffold that is infiltrated with an interpenetrating network hydrogel can build a functional biomaterial that provides the load-bearing and tribological properties of native cartilage. An interpenetrating dual-network "tough-gel" consisting of alginate and polyacrylamide was infused into a porous three-dimensionally woven poly(ε-caprolactone) fiber scaffold, providing a versatile fiber-reinforced composite structure as a potential acellular or cell-based replacement for cartilage repair.

1. Introduction

Articular cartilage is the thin, load-bearing connective tissue covering the ends of long bones in diarthrodial joints. Under normal conditions, this inhomogeneous, anisotropic, multiphasic, and viscoelastic tissue provides a smooth, lubricated surface for articulation, facilitates load support of up to multiple times body weight, dissipates energy, and effectively transfers motions between the bones of the skeleton.[1] The unique composition and structure of this tissue are responsible for its complex mechanical properties, which effectively allow the tissue to function as a nearly frictionless bearing surface over decades of life, with little or no wear under normal circumstances.[2] More specifically, it is this composition and structural organization that governs its mechanical response to stress by giving rise to critical pressurization of the interstitial fluid as it physically interacts with the solid matrix constituents, namely collagen and proteoglycans.[3–5] Damage to this tissue leads to the loss of mechanical function and progressive osteoarthritic degeneration, resulting in significant pain and disability.[6]

In this regard, the engineered repair or regeneration of cartilage remains an important goal for treating cartilage injury or osteoarthritis. Many strategies for developing tissue-engineered cartilage have used hydrogels as cell carriers, or as biomechanical tissue replacements.[7] In general, these hydrogels have very high water content (e.g., >90 wt%), can be readily seeded with cells, and support the formation of an extracellular matrix (ECM) (reviewed elsewhere).[8,9] Although such hydrogels can be highly conducive for chondrogenesis by primary chondrocytes or stem/progenitor cells, it has proven difficult to effectively recreate both the biomechanical and biochemical functions of the natural tissue in short-term culture. Commonly used hydrogels, such as agarose, alginate, hyaluronic acid, or poly(ethylene glycol) (PEG), generally consist of polymers of single networks and exhibit relatively low stiffness and wear properties, even after many weeks of culture.[10–16] However, recreating the mechanical properties of healthy articular cartilage is of great importance as the initial (pre-implantation) mechanical properties of an implantable construct must provide the ability to withstand physiologic joint loading,[17] which results in contact stresses reaching several megapascals.[18] The ability of native cartilage to withstand such magnitudes of stress is dependent upon the ability of the tissue to generate high interstitial fluid pressures due to its complex nonlinear and biphasic (fluid/solid) properties, allowing greater than 95% of the stress to be carried by the fluid phase of the material.[5]

To address the harsh biomechanical environment in the joint, there have been many studies aimed at enhancing the properties of hydrogels to be used as acellular, joint bearing materials.[19–21] For example, hydrogels of interpenetrating networks (IPN), which consist of two different polymers that are mixed with one another at the molecular scale, are especially attractive over their single network counterparts as they exhibit synergistically increased fracture toughness and tribological properties as compared to the individual components of the network.[22–29]WW In particular, a special type of IPN hydrogel was recently developed, in which one network of the hydrogel is crosslinked covalently and the other ionically.[29] The ionically-crosslinked network is capable of dissipating

Dr. I.-C. Liao, Dr. F. T. Moutos, Dr. B. T. Estes, Dr. F. Guilak
Department of Orthopaedic Surgery
Duke University Medical Center
Durham, NC 27710, USA
E-mail: guilak@duke.edu
Dr. X. Zhao, Dr. F. Guilak
Department of Mechanical Engineering and Materials Science
Duke University Medical Center
Durham, NC 27708, USA
E-mail: xz69@duke.edu

DOI: 10.1002/adfm.201300483

mechanical energy from external loads via reversible breaking of the crosslinks, while the covalently-crosslinked network maintains the shape of the hydrogel after deformation. As a result, the dual-polymer IPN has effective mechanical properties that are far superior to what would be assumed from the additive properties of the two separate network components. In addition, the IPN hydrogel can also form a charged outer surface, which is capable of maintaining a boundary water layer under high normal loads. This phenomenon effectively decreases the coefficient of friction of the material.[30] and is especially advantageous for cartilage tissue engineering applications.[5] Optimized IPN structures have been shown to increase maximum compressive stresses over single network hydrogels up to two orders of magnitude, while lowering the coefficient of friction to the same order as articular cartilage.[25,28,31,32] Realizing the mechanical benefits of assembling IPN gels, several studies have reported their use for cartilage tissue engineering. Most recently, the combination of agarose and poly(ethylene glycol) diacrylate resulted in an IPN with improved mechanical properties over single network hydrogels, with high viability of chondrocytes encapsulated within the gel.[26,27] In an in vivo study, an IPN gel (poly(2-acrylamido-2-methylpropanesulfonic acid) and poly(N,N′-dimethylacrylamide)) supported healing of an osteochondral defect when used as a substrate filler for tissue engineered repair of rabbit osteochondral defect.[24]

While such IPN hydrogels can provide significantly improved compressive and wear properties over single network hydrogels, the complex load bearing characteristics of native cartilage are dependent on inherent high tension–compression nonlinearity that allows rapid fluid pressurization under joint loading. In this regard, three-dimensionally woven fiber scaffolds have been shown to mimic many of the mechanical properties of articular cartilage materials by weaving fibers made of polyglycolic acid (PGA), polypropylene (prototype for a non-resorbable fiber), or poly(ε-caprolactone) (PCL).[33–36] The advantage of using a 3D woven structure is that it can be designed to match the nonlinear, inhomogenous, and anisotropic properties of cartilage prior to seeding with any cells, thereby making it suitable for immediate implantation.[33,37] These 3D woven fiber scaffolds have been tested with and without infiltration of various single network hydrogel matrices such as agarose, fibrin, alginate, or matrigel to create biomimetic fiber-reinforced composites.[33–36] While these hydrogels provide a chondroinductive environment for stem cell differentiation, they do not have sufficient mechanical properties for immediate implantation within the joint due to their brittle nature and low strength.

2. Results and Discussion

In this study, we hypothesized that a novel composite material made by infiltration of a 3D woven PCL scaffold with an IPN hydrogel would result in significant improvements in the mechanical and tribological properties over the 3D woven PCL scaffold or IPN alone. Interpenetrating network hydrogels using combinations of alginate (Alg), fibrin (Fib), and polyacrylamide (PAAm) were synthesized to evaluate their potential as candidates for synthetic articular cartilage. These hydrogels were chosen for their cellular and tissue biocompatibility and mechanical properties.[9,28,38–42] Unconfined compression, confined compression, dynamic unconfined compression, and friction tests were utilized to determine the mechanical properties of the hydrogels. The 3D woven PCL scaffold infiltrated with an Alg/PAAm IPN exhibited significant improvement in strain recovery (i.e., lower plastic deformation) relative to the 3D woven PCL scaffold alone, approaching that of articular cartilage and the IPN alone (**Figure 1**A). Without the contribution of the 3D woven PCL scaffold, the stress-strain behavior of the Alg/PAAm IPN hydrogel in unconfined compression exhibited classical IPN behavior, with significant increase in modulus over their single network counterparts (Figure 1B). At 10% strain, the Alg/PAAm IPN hydrogel showed approximately four times the Young's modulus of single network hydrogels of PAAm and Alg (0.22 MPa vs 0.05 MPa, Figure 1C). Fib/PAAm IPN hydrogels, however, did not exhibit the same mechanically enhanced properties as the Alg/PAAm hydrogels. The stress-strain constitutive relationship of Fib/PAAm hydrogels was similar to that of single network PAAm hydrogels with similar Young's modulus values of 0.052 and 0.047 MPa for Fib/PAAm and PAAm hydrogels, respectively, suggesting that the PAAm dominated the stress-strain response of this IPN (Figure 1B,C). In addition, the PAAm based single network and IPN networks (Alg/PAAm, Fib/PAAm) exhibited 3-fold decrease in their frictional properties as compared to Alg and Fib single network hydrogels (Figure 1D).

The significant improvements in the compressive and frictional properties of PAAm-based IPN hydrogels thus encouraged the investigation of infusing the IPN hydrogels into 3D woven PCL scaffolds to form anisotropic, nonlinear composites capable of serving as a synthetic scaffold for articular cartilage or for the purposes of articular cartilage tissue engineering. The hydrogels were evenly infused into the 3D woven scaffolds using a vacuum infusion technique, thereby producing a 3D woven PCL/IPN composite (**Figure 2**D–F). The 3D woven scaffold used in this work consisted of 7 layers of *x* and *y* fiber bundles of PCL with an average pore size of approximately 350 μm × 250 μm × 100 μm.[37] These stacked layers were interlocked with a third set of PCL fibers (*z*-direction) that were passed vertically through the layers following a continuous, repeated path (Figure 2A). Infusion of the scaffold with an IPN also served to minimize the surface roughness of the scaffold while improving the frictional properties of the composite. Infusion of the scaffold with the IPN reduced the surface roughness by approximately 80% (23.6 μm for the scaffold to 5.2 μm for the IPN composite, Figure 2B vs Figure 2E).

The 3D woven PCL scaffold alone (labeled "scaffold" in the figures) exhibited an average Young's modulus of 0.1 MPa (**Figure 3**A). The infusion of alginate or fibrin single network hydrogels did not significantly alter the modulus of the composite, indicating that the scaffold component of the composite served as the main determinant of the modulus in these cases (Figure 3A). Infusion of the 3D woven PCL scaffold with IPNs of Alg/PAAm or Fib/PAAm significantly increased the Young's modulus over the PCL scaffold alone. Specifically, the aggregate modulus of the Alg/PAAm IPN (≈0.4 MPa) was significantly higher than that of the single network hydrogel of alginate or PAAm separately (Figure 3B). However, the reinforcement of the hydrogel with the 3D woven scaffold resulted in a further

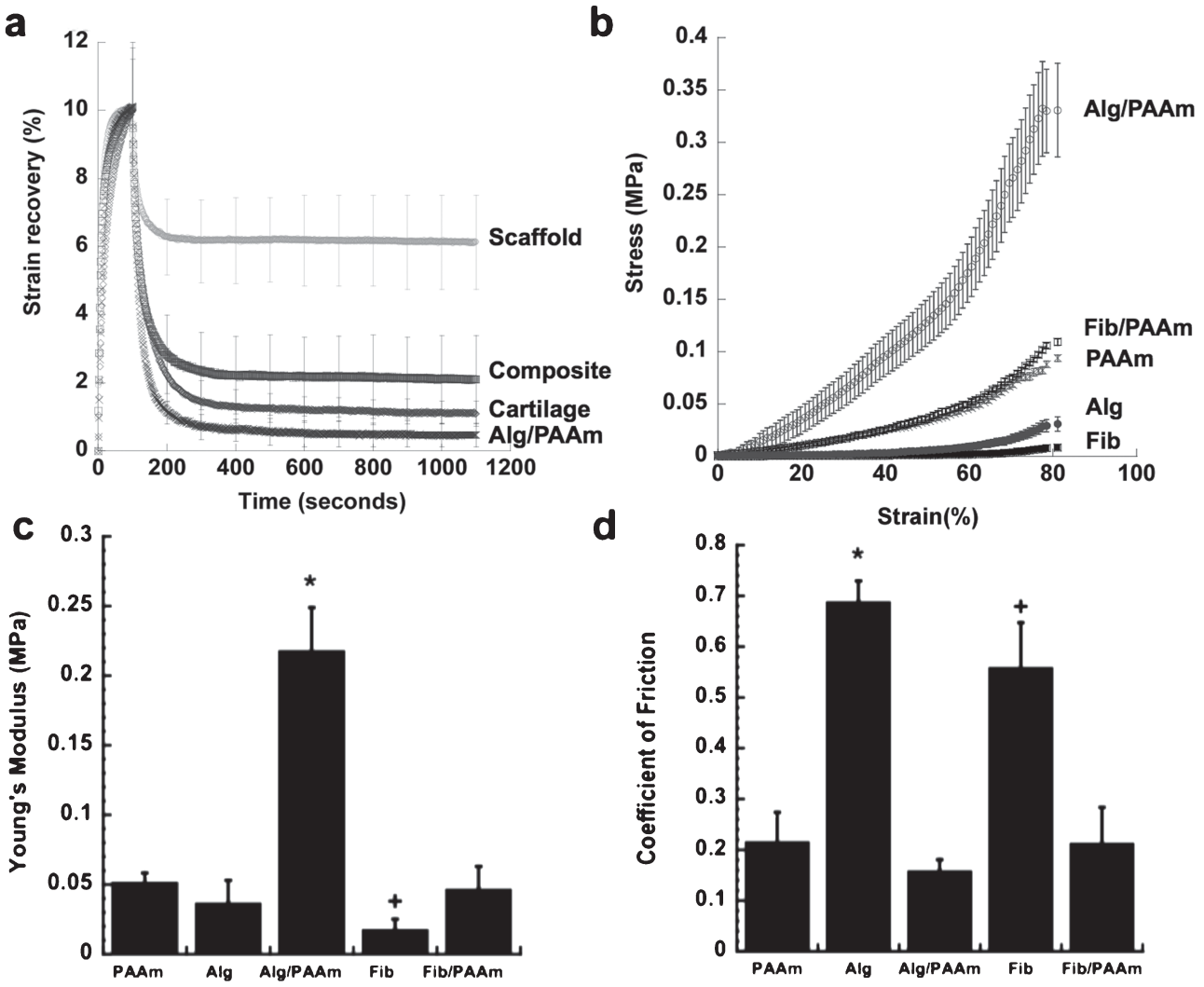

Figure 1. Compressive and frictional properties of IPN hydrogels. PAAm = polyacrylamide, Alg = alginate, Fib = fibrin, Alg/PAAm = alginate/polyacrylamide, and Fib/PAAm = fibrin/polyacrylamide. A) PCL scaffold alone, PCL/Alg/PAAm-IPN composite, cartilage, and Alg/PAAm strain recovery following 10% strain. B) Stress-strain behavior of the hydrogels during compression. C) Young's modulus of the hydrogels calculated from unconfined compression studies. $*p < 0.05$ for Alg/PAAm vs PAAm, Alg, Fib, and Fib/PAAm. $+p < 0.05$ for Fib/PAAm vs PAAm and Fib. D) Coefficient of friction of the hydrogels determined using a rheometer. $*p < 0.05$ for Alg vs Alg/PAAm, Alg, and Fib/PAAm. $+p < 0.05$ for Fib vs PAAm, Alg/PAAm, and Fib/PAAm.

improvement in the modulus of the composite construct, with values reaching approximately 1.2 MPa for 3D woven PCL infiltrated with Alg/PAAm IPN and 0.9 MPa for the 3D woven PCL infiltrated with Fib/PAAm IPNs (Figure 3B). Single network hydrogel/3D woven PCL composites exhibited an aggregate modulus similar to that of the 3D woven PCL scaffold alone (Figure 3B), suggesting that the PCL scaffold primarily determines the properties of these single-network composites. On the other hand, the moduli for the IPN hydrogel/PCL composites were significantly higher than the PCL scaffold alone (Figure 3B). In the case of the composite 3D woven PCL scaffold infiltrated with Alg/PAAm, the modulus was approximately twice the value measured in the 3D woven PCL scaffolds alone (1.25 vs 0.69 MPa). This finding suggests that the interaction of the IPN hydrogels with the 3D woven PCL scaffold was responsible for the improvement in mechanical strength, a departure from conventional interpretation of fiber reinforced gel networks, in which the fiber components generally serve as the strength determinant.[37]

We also measured the dynamic moduli of the hydrogels and composites and compared the values to those of native cartilage as a measure of the scaffold response to cyclic loading that occurs in vivo (Figure 3C,D).[4,43–45] Porcine articular cartilage (from the femoral condyle), used as a positive control in our testing, demonstrated dynamic moduli ranging from approximately 10 MPa to 22 MPa at 0.1 and 10 Hz, respectively. These properties are in the range of previously reported values for human and bovine articular cartilage, ranging from 14–60 MPa, depending on the loading frequency.[45–47] Dynamic moduli for Alg/PAAm IPNs were relatively low, averaging 0.8 MPa across

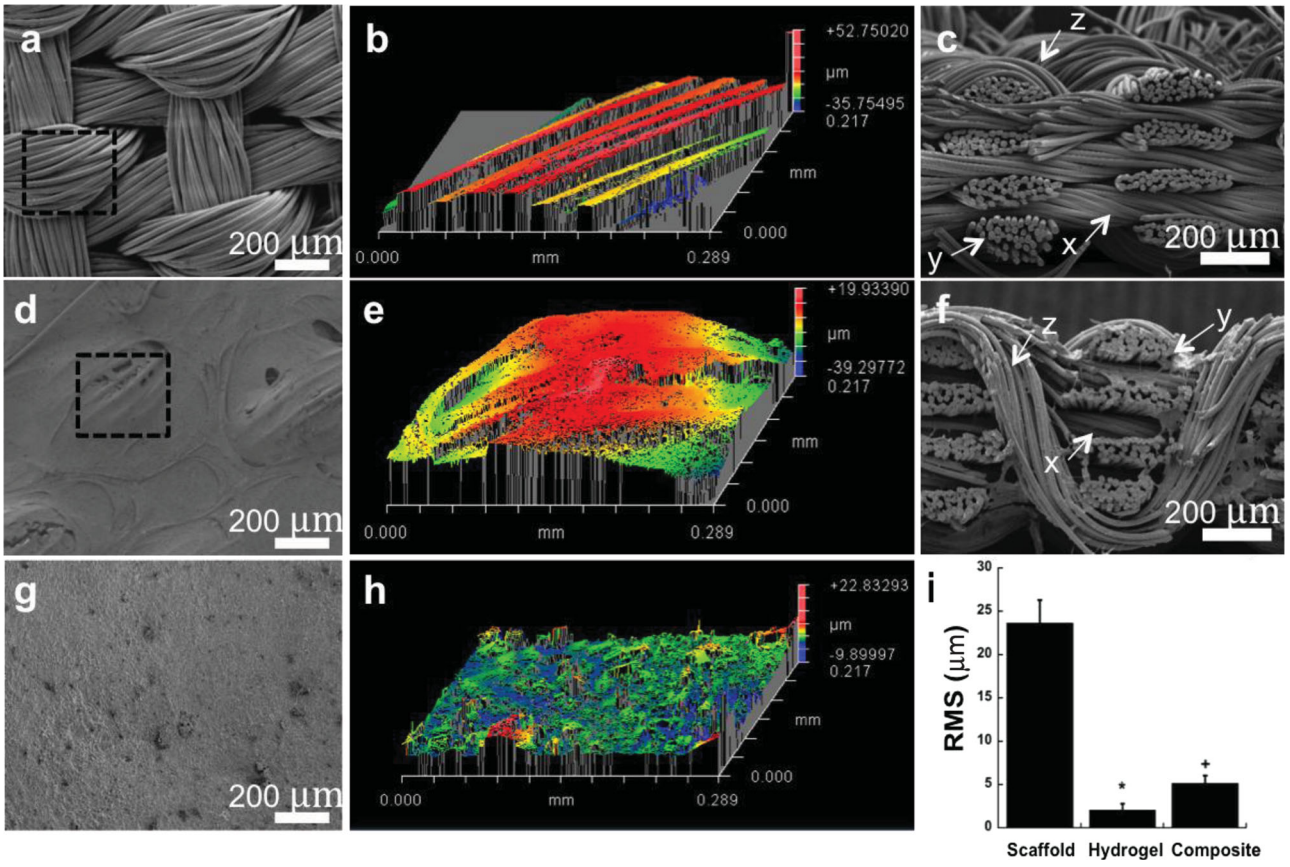

Figure 2. A,B) Scanning electron microscopy (SEM) images and 3D optical profiles of 3D woven PCL scaffold surface. Outlined area in panel A denotes total scanned area in panel B. C) Cross-sectional image of 3D woven PCL scaffold. D,E) SEM and 3D optical profile of 3D woven PCL-Alg/PAAm IPN composite surface. Outlined area in panel D denotes total scanned area in panel E. F) Cross-sectional image of 3D woven PCL-Alg/PAAm IPN composite scaffold. G,H) SEM and 3D optical profile of Alg/PAAm IPN surface. I) Average RMS of the 3D woven PCL scaffold (scaffold), Alg/PAAm IPN (hydrogel), and 3D woven PCL-Alg/PAAm IPN composite (composite) constructs. $*p < 0.05$ for hydrogel vs scaffold, and composite. $+p < 0.05$ for composite vs scaffold and hydrogel. All scale bars = 200 µm.

all compression frequencies, due to the relatively low cross-link densities of the IPNs and high water concentration in the hydrogel. The 3D woven PCL scaffold alone also performed well at low frequencies, but did not exhibit increased moduli at higher frequencies (10 Hz), presumably due to the inability to generate interstitial fluid pressurization within the large open pore structure of the matrix[5] (Figure 3D). Conversely, even though the composite 3D woven PCL-Alg/PAAm constructs did not reach the dynamic modulus of native articular cartilage, it showed a marked increase in dynamic moduli at high frequencies, since the infiltration of the IPN hydrogel enables the interstitial fluid pressurization within the PCL scaffold matrix. This increase in dynamic moduli at high frequencies represents a noteworthy improvement in the mechanical properties of the fiber-based composite over the 3D woven PCL scaffold or IPN hydrogels by themselves (Figure 3C,D).

As the bearing surface for the synovial joints of the body, articular cartilage is subjected to millions of loading cycles, while providing an extremely low coefficient of friction.[5] The coefficient of friction of the 3D woven PCL scaffold, tested against a native cartilage surface, was 0.64 ± 0.11. By infusing the 3D woven PCL scaffold with the Alg/PAAm IPN hydrogel, the coefficient of friction was significantly reduced to 0.28 ± 0.05 (**Figure 4**), which is similar to previously reported values for articular cartilage (0.2).[35]

3. Conclusions

This study introduces the concept of infusing a mechanically robust interpenetrating network hydrogel into highly structured 3D woven fibrous scaffolds as a means of creating a synthetic material that has tunable mechanical and tribological properties that mimic those of native cartilage. The IPN hydrogel composites showed significant improvements in the Young's aggregate and dynamic moduli over the constituent scaffold or hydrogels alone. The measured compressive properties of the 3D woven PCL-Alg/PAAm IPN composite compared favorably with published values of articular cartilage explants (0.4 MPa for Young's modulus and 1 MPa for aggregate modulus). In unconfined compression, the stress-strain behavior of the composite showed significant improvement over Alg/PAAm IPN hydrogel or 3D woven PCL scaffold alone, and showed a similar behavior qualitatively to that of native articular cartilage (Figure 3C). The IPN hydrogels and composites in this study also exhibited low coefficients of

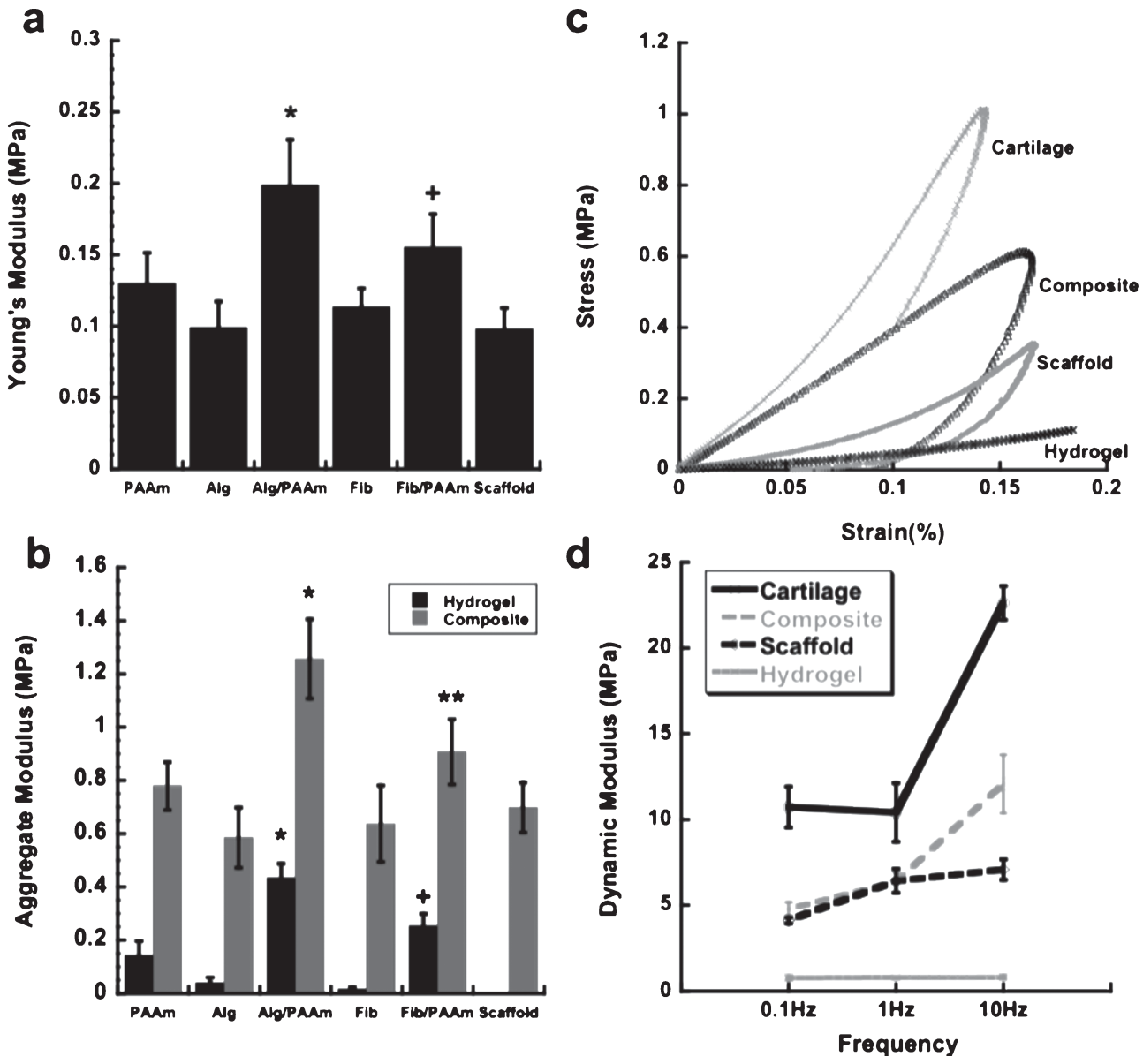

Figure 3. A) Young's modulus of the PCL scaffold alone and the IPN hydrogel composites (all groups in this plot contain the PCL scaffold, the hydrogel was infused in the PCL scaffold to create the composite). $*p < 0.05$ for Alg/PAAm vs all groups except Fib/PAAm. $+p < 0.05$ for Fib/PAAm vs all groups except Alg/PAAm. B) Aggregate modulus of IPN and single network hydrogels and their combination with the PCL scaffold to form composites. $*p < 0.05$ for Alg/PAAm composite vs all groups. $+p < 0.05$ for Fib/AAM hydrogel vs all groups. $**p < 0.05$ for Fib/PAAm composite vs Alg and Fib composites and scaffold alone. C) Stress-strain behavior and D) dynamic moduli of porcine articular cartilage, Alg/PAAm hydrogel, Alg/PAAm composite, and woven scaffold.

friction similar to native cartilage explants. Importantly, other IPN combinations may provide novel biological as well as biomechanical properties. For example, recent studies have shown that Alg/Fib hydrogels, despite showing a reduced compressive modulus, exhibited significantly improved cellular infiltration and vascular ingrowth in an in vivo soft tissue repair model, as compared to either component alone.[48] Ongoing development of this synthetic scaffold technology will require the evaluation of long term wear simulation tests and the assessment of implant integration and stability over time in animal studies.

4. Experimental Section

Acrylamide hydrogels were produced by first mixing 50 wt% acrylamide (A3553, Sigma) in distilled H_2O, followed by adding 60 µL of 2.5 wt% N,N′-Methylenebis-acrylamide (MBAA, 146072, Sigma), 2 µL of N,N,N′,N′-Tetramethylethylenediamine (TEMED, T9281, Sigma), and 60 µL of 10% ammonium persulfate (AP, A3678, Sigma). The acrylamide solution was mixed and cast into the round circular molds for 30 min to obtain hydrogels of uniform thickness. The final concentrations of the various components were 44.56% acrylamide, 0.15% MBAA, 0.6% AP, 0.178% TEMED. Alginate hydrogels were produced by casting 2 wt% alginate solution (A2158, Sigma) into circular molds followed by excess

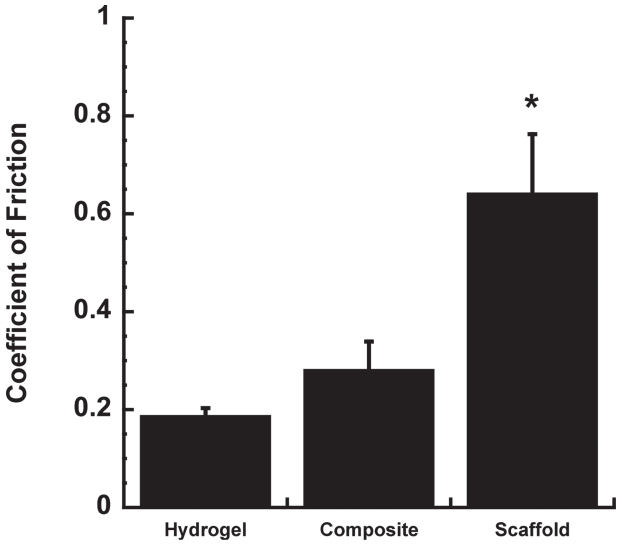

Figure 4. The equilibrium coefficient of friction of different constructs tested against native articular cartilage. 3D woven PCL scaffold showed a relatively high coefficient of friction, whereas the Alg/PAAm IPN composite and Alg/PAAm hydrogel showed significantly lower coefficients of friction. $*p < 0.05$ for 3D woven PCL scaffold vs hydrogel and composite.

amount of 10% $CaCl_2$ solution. The alginate hydrogels were left in the $CaCl_2$ solution for 1 h to ensure complete crosslinking throughout the gel. Fibrin hydrogels were produced by dissolving 50 mg of fibrinogen (F 3879, Sigma) in 1 mL of 1% NaCl solution followed by adding thrombin (T6884, 500 U/mL, Sigma) in a 1:10 volume ratio of thrombin: fibrinogen. The fibrin hydrogels were allowed to solidify for 1 h prior to transferring into phosphate buffered solutions. Interpenetrating network hydrogels of Alg/PAAm were produced by dissolving 2% alginate and 50% acrylamide in distilled H_2O, followed by the same protocol used to create acrylamide hydrogel. After 30 min of crosslinking the acrylamide component, the hydrogel was transferred into a 10% $CaCl_2$ solution for 1 h to crosslink the alginate hydrogel network. The hydrogel was then transferred into a bath of distilled H_2O for 1 h, followed by phosphate buffered saline (PBS) solution for long-term storage in 4 °C. In a similar fashion, Fib/PAAm IPN hydrogels were produced by mixing fibrinogen and acrylamide in 1% NaCl solution. After adding 60 µL of 2.5 wt% MBAA and 60 µL of 40 wt% AP solutions, a 1:10 volume ratio of 500 U/mL thrombin solution and 2 µL of TEMED solution were added and mixed well to simultaneously crosslink both networks. The solutions were allowed to stand still for 1 h in room temperature prior to transferring into PBS solutions.

To engineer the 3D woven fiber scaffold used in this work, we employed a previously described experimental setup which adapts linear motors to weave PCL yarns into woven structures that consisted of yarns in *x*, *y*, and *z* directions.[35,37] The woven construct was approximately 800 µm thick with average pore size of 350 µm × 250 µm × 100 µm. A previously described vacuum infusion technique was used to infuse the hydrogels into the 3D woven scaffold.[35] Briefly, an elastic film was placed over the woven scaffolds followed by creating a vacuum seal around the construct. The hydrogel mixture was initiated to crosslink then injected into the vacuum bag immediately. The pressure gradient driven by the vacuum seal thus evenly distributed the injected hydrogels into the woven construct. Similar to the hydrogel production, the composites were allowed to solidify in PBS solution prior to storage. To evaluate the samples under SEM (scanning electron microscope, FEI XL30, FEI) and Zygo optical profiler (Zygo NewView 5000, Zygo), all samples (with exception of the already dry woven scaffolds) underwent serial dehydration to 100% ethanol followed by chemical drying using hexamethyldisilizane. The dried samples were gold coated prior to mounting on stubs for SEM and Zygo profiler imaging. Root mean square (RMS) values for surface roughness were determined by taking 50 measurements from 5 individual samples in each group and an average sampling area of 0.067 mm^2.

For all mechanical experiments, the test samples were punched into 3 mm diameter circular discs. All compression tests were carried out on an ELF 3200 series precision controlled materials testing system (Bose, Minnetonka, MN). For unconfined compression tests, a 0.03 N tare load (0.01 N tare load for hydrogels) was first placed on the scaffolds and the composites. The samples were allowed to equilibrate, followed by subsequent strains of 0.04, 0.08, and 0.12. Each step strain was held constant for 600 s to allow the samples to equilibrate, and the Young's modulus was determined by linear regression of the resultant stress strain curve. The aggregate modulus was determined using a confined compression configuration, where the samples were placed in a 3 mm diameter confining chamber. After equilibrating with 0.03 N tare load, a step compressive load of 0.15 N was applied to the samples and allowed to equilibrate over 1500 s. The compressive aggregate modulus was determined using a three parameter, nonlinear least squares regression assuming intrinsic incompressibility of the constituents.[49,50] The dynamic moduli of the samples were determined according to a previously reported procedure.[45] The samples tested in this study were equilibrated under a 0.4 N tare load, followed by cyclic loading of 0.1, 1, and 10 Hz to 20% strain. All samples were allowed 1000 s to relax between tests. Friction tests were performed according to previously published procedures using an AR-G2 rheometer (TA Instruments).[3] All testing groups in this study consisted of 5 individual samples, and the statistical significance between the groups was determined by one way ANOVA followed by Tukey-Kramer HSD test. Samples with $p < 0.05$ were determined to be statistically significant.

Acknowledgements

This work was supported in part by National Institutes of Health grants AG15768, AR50245, AR48182, AR48852, the Arthritis Foundation, the Collaborative Research Center, AO Foundation, Davos, Switzerland and the NSF (CMMI-1253495, CMMI-1200515, and DMR-1121107). The authors thank Dr. Jeffrey Coles, Dr. Stefan Zauscher, Hiral Tailor, and Julia Weidner for their intellectual and experimental contributions.

Received: February 5, 2013
Revised: April 6, 2013
Published online: June 27, 2013

[1] V. C. Mow, A. Ratcliffe, A. R. Poole, *Biomaterials* **1992**, *13*, 67.
[2] F. Guilak, L. A. Setton, V. B. Kraus, in *Principles and Practice of Orthopaedic Sports Medicine* (Eds: W. E. Garrett, K. Speer, D. Kirkendall), Lippincott Williams and Wilkins, Philadelphia **2000**, 53.
[3] H. Q. Wang, G. A. Ateshian, *J. Biomech.* **1997**, *30*, 771.
[4] M. A. Soltz, G. A. Ateshian, *Ann. Biomed. Eng.* **2000**, *28*, 150.
[5] G. A. Ateshian, *J. Biomech.* **2009**, *42*, 1163.
[6] A. Praemer, S. Furner, D. P. Rice, *Musculoskeletal Conditions in the United States*, American Academy of Orthopaedic Surgeons, Rosemont, IL **1999**.
[7] H. Awad, G. R. Erickson, F. Guilak, in *Tissue engineering and biodegradable equivalents: scientific and clinical applications*, (Eds: K. Lewandrowski, D. Wise, D. Trantolo, J. Gresser, M. Yaszemski, D. Altobelli), Marcel Dekker, New York **2002**, p. 267.
[8] K. Y. Lee, D. J. Mooney, *Chem. Rev.* **2001**, *101*, 1869.
[9] J. L. Drury, D. J. Mooney, *Biomaterials* **2003**, *24*, 4337.
[10] H. A. Awad, M. Q. Wickham, H. A. Leddy, J. M. Gimble, F. Guilak, *Biomaterials* **2004**, *25*, 3211.
[11] C. Chung, M. Beecham, R. L. Mauck, J. A. Burdick, *Biomaterials* **2009**, *30*, 4287.

[12] I. E. Erickson, A. H. Huang, C. Chung, R. T. Li, J. A. Burdick, R. L. Mauck, *Tissue Eng., Part A* **2009**, *15*, 1041.
[13] I. E. Erickson, A. H. Huang, S. Sengupta, S. Kestle, J. A. Burdick, R. L. Mauck, *Osteoarthritis Cartilage* **2009**, *17*, 1639.
[14] S. Hofmann, S. Knecht, R. Langer, D. L. Kaplan, G. Vunjak-Novakovic, H. P. Merkle, L. Meinel, *Tissue Eng.* **2006**, *12*, 2729.
[15] A. H. Huang, A. Stein, R. S. Tuan, R. L. Mauck, *Tissue Eng., Part A* **2009**, *15*, 3461.
[16] R. L. Mauck, X. Yuan, R. S. Tuan, *Osteoarthritis Cartilage* **2006**, *14*, 179.
[17] F. Guilak, D. L. Butler, S. A. Goldstein, *Clin. Orthop. Relat. Res.* **2001**, S295.
[18] T. D. Brown, D. T. Shaw, *J. Biomech.* **1983**, *16*, 373.
[19] M. Oka, Y. S. Chang, T. Nakamura, K. Ushio, J. Togochida, H. O. Gu, *J. Bone Jt. Surg.: Br. Vol.* **1997**, *79B*, 1003.
[20] M. E. Freeman, M. J. Furey, B. J. Love, J. M. Hampton, *Wear* **2000**, *241*, 129.
[21] H. Bodugoz-Senturk, C. E. Macias, J. H. Kung, O. K. Muratoglu, *Biomaterials* **2009**, *30*, 589.
[22] M. Kobayashi, J. Toguchida, M. Oka, *Biomaterials* **2003**, *24*, 639.
[23] S. L. Riley, S. Dutt, R. de la Torre, A. C. Chen, R. L. Sah, A. Ratcliffe, *J. Mater. Sci.: Mater. Med.* **2001**, *12*, 983.
[24] K. Yasuda, N. Kitamura, J. P. Gong, K. Arakaki, H. J. Kwon, S. Onodera, Y. M. Chen, T. Kurokawa, F. Kanaya, Y. Ohmiya, Y. Osada, *Macromol. Biosci.* **2009**, *9*, 307.
[25] K. Yasuda, J. P. Gong, Y. Katsuyama, A. Nakayama, Y. Tanabe, E. Kondo, M. Ueno, Y. Osada, *Biomaterials* **2005**, *26*, 4468.
[26] B. J. DeKosky, N. H. Dormer, G. C. Ingavle, C. H. Roatch, J. Lomakin, M. S. Detamore, S. H. Gehrke, *Tissue Eng., Part C* **2010**, *16*, 1533.
[27] G. C. Ingavle, N. H. Dormer, S. H. Gehrke, M. S. Detamore, *J. Mater. Sci.: Mater. Med.* **2012**, *23*,157.
[28] J. P. Gong, Y. Katsuyama, T. Kurokawa, Y. Osada, *Adv. Mater.* **2003**, *15*, 1155.
[29] J. Y. Sun, X. Zhao, W. R. Illeperuma, O. Chaudhuri, K. H. Oh, D. J. Mooney, J. J. Vlassak, Z. Suo, *Nature* **2012**, *489*, 133.
[30] J. P. Gong, T. Kurokawa, T. Narita, G. Kagata, Y. Osada, G. Nishimura, M. Kinjo, *J. Am. Chem. Soc.* **2001**, *123*, 5582.
[31] D. Myung, D. Waters, M. Wiseman, P. E. Duhamel, J. Noolandi, C. N. Ta, C. W. Frank, *Polym. Adv. Technol.* **2008**, *19*, 647.
[32] H. Omidian, J. G. Rocca, K. Park, *Macromol. Biosci.* **2006**, *6*, 703.
[33] F. T. Moutos, B. T. Estes, F. Guilak, *Macromol. Biosci.* **2010**, *10*, 1355.
[34] F. T. Moutos, F. Guilak, *Biorheology* **2008**, *45*, 501.
[35] F. T. Moutos, F. Guilak, *Tissue Eng., Part A* **2010**, *16*, 1291.
[36] P. K. Valonen, F. T. Moutos, A. Kusanagi, M. G. Moretti, B. O. Diekman, J. F. Welter, A. I. Caplan, F. Guilak, L. E. Freed, *Biomaterials* **2010**, *31*, 2193.
[37] F. T. Moutos, L. E. Freed, F. Guilak, *Nat. Mater.* **2007**, *6*, 162.
[38] A. D. Augst, H. J. Kong, D. J. Mooney, *Macromol. Biosci.* **2006**, *6*, 623.
[39] J. Patterson, M. l. M. Martino, J. A. Hubbell, *Mater. Today* **2010**, *13*, 14.
[40] Y.-H. Na, T. Kurokawa, Y. Katsuyama, H. Tsukeshiba, J. P. Gong, Y. Osada, S. Okabe, T. Karino, M. Shibayama, *Macromolecules* **2004**, *37*, 5370.
[41] C. Azuma, K. Yasuda, Y. Tanabe, H. Taniguro, F. Kanaya, A. Nakayama, Y. M. Chen, J. P. Gong, Y. Osada, *J. Biomed. Mater. Res., Part A* **2007**, *81A*, 373.
[42] T. Kurokawa, H. Furukawa, W. Wang, Y. Tanaka, J. P. Gong, *Acta Biomater.* **2010**, *6*, 1353.
[43] C. Y. Huang, V. C. Mow, G. A. Ateshian, *J. Biomech. Eng.* **2001**, *123*, 410.
[44] R. C. Lee, E. H. Frank, A. J. Grodzinsky, D. K. Roylance, *J. Biomech. Eng.* **1981**, *103*, 280.
[45] S. Park, C. T. Hung, G. A. Ateshian, *Osteoarthritis Cartilage* **2004**, *12*, 65.
[46] L. Bian, E. G. Lima, S. L. Angione, K. W. Ng, D. Y. Williams, D. Xu, A. M. Stoker, J. L. Cook, G. A. Ateshian, C. T. Hung, *J. Biomech.* **2008**, *41*, 1153.
[47] J. Kinnunen, S. Saarakkala, M. Hauta-Kasari, P. Vahimaa, J. S. Jurvelin, *Biomed. Opt. Express* **2011**, *2*, 1394.
[48] C. M. Hwang, B. Ay, D. L. Kaplan, J. P. Rubin, K. G. Marra, A. Atala, J. J. Yoo, S. J. Lee, *Biomed. Mater.* **2013**, *8*, 014105.
[49] V. C. Mow, S. C. Kuei, W. M. Lai, C. G. Armstrong, *J. Biomech. Eng.* **1980**, *102*, 73.
[50] N. M. Bachrach, V. C. Mow, F. Guilak, *J. Biomech.* **1998**, *31*, 445.